0013-7227/01/$03.00/0
Endocrinology

Vol. 142, No. 5
Printed in U.S.A.

Synchronized Exocytotic Bursts from Gonadotropin-Releasing Hormone-Expressing Cells: Dual Control by Intrinsic Cellular Pulsatility and Gap Junctional Communication*

RAFAEL VAZQUEZ-MARTINEZ, SPENCER L. SHORTE, FREDRIC R. BOOCKFOR, AND L. STEPHEN FRAWLEY

Laboratory of Molecular Dynamics, Department of Cell Biology and Anatomy, Medical University of South Carolina, Charleston, South Carolina 29425

ABSTRACT

Periodic secretion of GnRH from the hypothalamus is the driving force for the release of gonadotropic hormones from the pituitary, but the roles of individual neurons in the context of this pulse generator are not known. In this study we used FM1–43 to monitor the membrane turnover associated with exocytosis in single GT1–7 neurons and found an intrinsic secretory pulsatility (frequency, 1.4 ± 0.1/h; pulse duration, 17.3 ± 0.6 min) that, during time in culture, became progressively synchronized among neighboring cells. Voltage-gated calcium channels and gap junctional communication each played a major role in synchronized pulsatility. An L-type calcium channel inhibitor, nimodipine, abolished synchronized pulsatility. In addition, functional gap junction communication among adjacent cells was detected, but only under conditions where pulsatile synchronization was also observed, and the gap junction inhibitor octanol abolished both without affecting pulse frequency or duration. Our results, therefore, provide strong evidence that the GnRH pulse generator in GT1–7 cells arises from a single cell oscillator mechanism that is synchronized through network signaling involving voltage-gated calcium channels and gap junctions. (*Endocrinology* **142:** 2095–2101, 2001)

IT IS WELL recognized that periodic release of GnRH from the hypothalamus controls the episodic secretion of LH from the anterior pituitary. Because this phenomenon is central to reproductive function in mammals (1), the cellular mechanisms governing GnRH pulsatility have been the focus of extensive study (2). It was found that GnRH release from isolated hypothalamic fragments was episodic, indicating that the phenomenon is initiated in the absence of extrahypothalamic input (1, 2). Inasmuch as GnRH neurons are organized into an interconnected network diffusely distributed throughout the hypothalamus (3), it has been hypothesized that episodic secretion must arise from a GnRH pulse generator that synchronizes the activity of individual cells within this neuronal network (4). Understanding the GnRH pulse generator requires knowledge of how pulsatile secretory dynamics in single neurons are related to the secretory dynamics of neuronal cell populations.

An important advance in our understanding of the cellular basis for GnRH pulsatility was the finding that GnRH release from populations of GT1 clones, immortalized mouse GnRH neurons (5), was episodic (6–10) with an interpulse interval comparable to that observed for primary cultures from castrated rodents (11). From this and other work, several groups have speculated that the pulse generator must reside at the level of either the neuronal network (6, 12, 13) or the individual cell (7–10). In the former scenario, it can be envisaged that individual cells might harbor the ability to release GnRH, but that this would lack an episodic dynamic in the absence of network connectivity. In the latter scenario, individual neurons might release GnRH in a pulsatile fashion, independent of their network connectivity. Unfortunately, there is currently little basis to distinguish between these possibilities because the available evidence for secretion has been derived entirely from cell populations that provide limited insight into the contribution of single cells to secretory dynamics.

Recently, Betz and colleagues adapted the use of FM1–43 for monitoring granule to plasma membrane fusion in living cells during exocytosis (14, 15). Upon fusion, the granule membranes become exposed to and are subsequently labeled by this fluorescent dye present in the culture medium. Much of this newly incorporated dye is internalized during the endocytotic vesicle formation that follows exocytosis. Thus, this dye provides an exceptional marker for membrane changes associated with the secretory process. In previous work we adapted this technique for use with individual GT1–7 cells (16). Our results demonstrated clearly that FM1–43 uptake was increased after treatment with GnRH stimulatory secretagogues and inhibited with exposure to an inhibitory secretagogue. These findings indicated that many of the changes in FM1–43 fluorescence reflect membrane changes associated with the secretory process in individual cells. In the current study we further confirmed that this technique can be used as a marker of exocytosis in single cells and determined the impact of cell-cell communication on GT1–7 pulsatile activity. This strategy enabled us to address

Received November 10, 2000.
Address all correspondence and requests for reprints to: Dr. L. Stephen Frawley, Laboratory of Molecular Dynamics, Department of Cell Biology and Anatomy, Medical University of South Carolina, 171 Ashley Avenue, Charleston, South Carolina 29425. E-mail: frawleys@musc.edu.
* This work was supported by NIH Grant HD-37657 (to L.S.F.).

the compelling issue of whether the pulse generator resides in the GT1–7 neuronal network or the individual neuron.

Materials and Methods

Cell cultures

GT1–7 cells (provided by Dr. Richard I. Weiner, University of California, San Francisco, CA) were cultured in high glucose DMEM supplemented with 10% FBS, 1% streptomycin/penicillin, and 1% fungizone. Unless indicated otherwise, all tissue culture supplies were obtained from Life Technologies, Inc. (Grand Island, NY). Cells were maintained at 37 C in a water-saturated atmosphere of 95% air and 5% CO_2, and medium was replenished every 48 h. Two to 7 days before experimentation, cells were detached from six-well plastic dishes by gentle treatment with 0.05% trypsin and 0.53 mM EDTA for 5 min at 37 C, and then cultured on Matrigel (Collaborative Biomedical Products, Bedford, MA)-coated, 25-mm round glass coverslips at a density of 12,500 cells/0.8 cm^2.

Monitoring of FM1–43 fluorescence

A mixture of medium 199 and DMEM/F-12 (1:1) supplemented with 1 mM HEPES and 1% streptomycin/penicillin was used as the imaging medium. After three rinses with this medium, cells were exposed to the fluorescent dye FM1–43 [*N*-(3-triethylammoniopropyl)-4-(*p*-dibutylaminostyryl piridinium dibromide, 2 μM; Molecular Probes, Inc., Eugene, OR] for 30 min at 37 C. The coverslips bearing the cells were then mounted in Sykes-Moore chambers (Bellco Glass, Inc., Vineland, NJ). The chambers were next placed on a temperature-controlled stage of a fluorescence microscope (Axiovert, Carl Zeiss, Jena, Germany) fitted with a Carl Zeiss Fluar ×40 oil immersion objective (numerical aperture = 0.9), and a field of cells was selected. Then cells were epi illuminated at 490 nm for 100–500 msec every 5 min for 2–25 h. Image acquisition was controlled using Metafluor PC-software (Universal Imaging Corp., West Chester, PA), and fluorescence emissions were captured using a CCD camera (C-4880–80, Hamamatsu, Hamamatsu City, Japan) running in 10-bit mode. The images acquired were transferred to off-line storage for analysis at a later time. Regions of the same field devoid of cells were selected for continuous monitoring of the background throughout each experiment. Inasmuch as the illumination intensity was reduced to less than 5% by placing filters in the light path, and the absorption spectrum of FM1–43 (490 nm) approached visible light, the phototoxic effects that prolonged exposure to light can induce were minimized. Treatments with nimodipine (0.1 μM in imaging medium) and octanol (20 μM in imaging medium) were performed 90 and 30 min before image acquisition, respectively. Nimodipine was maintained in the imaging medium throughout each experiment.

Evaluation of gap junction functionality

GT1–7 cells were plated onto Matrigel-coated, 25-mm coverslips that were photoengraved with an alpha-numeric grid pattern. These cultures were then incubated for 2–4 days or 5–7 days, after which selected cells (1–20/field) were microinjected with a dye mixture consisting of 1.25% Lucifer Yellow CH (LY; lithium salt; M_r, 457 Da; Molecular Probes, Inc.) and 1.25% rhodamine B-dextran (M_r, 10,000 Da; Molecular Probes, Inc.) in water. After excitation at 480 nm (for LY) and 550 nm (for rhodamine), microinjected cells were identified by their fluorescent emissions at both 528 nm (for LY) and 590 nm (for rhodamine). Gap junction functionality was estimated as the ratio (R) of the number of cells showing LY fluorescence to the number of cells exhibiting both LY and rhodamine fluorescence minus 1 [R = (LY/LY and rhodamine) − 1]. The rationale for subtracting 1 was to allow the degree of functionality to equal zero in instances where no intercellular transit of dye occurred.

Data analysis

Inasmuch as FM1–43 was maintained in the imaging medium for as long as the data were collected, the fluorescence signal tended to increase continuously. Increments in fluorescence are manifested in the fluorescent profile as stair-step increases in total signal. To demonstrate that these stepwise increases were actually reflective of exocytosis, we studied FM1–43 incorporation in cells in which fusion of granules to the cell membrane was blocked by cytoplasmic microinjection of 1 mg/ml mouse monoclonal antibody to SNAP-25 (SMI 81, Sternberger Monoclonals, Inc., Lutherville, MD). After loading with FM1–43, microinjected cells were identified by their fluorescent emission at 590 nm (for rhodamine dextran, which was coinjected with the antibody (1:1), and FM1–43 incorporation was monitored as described above. Cells injected with a nonspecific antibody (1 mg/ml mouse IgG1 κ; MOPC 21, Sigma-Aldrich Corp., St. Louis, MO) that presents the same isotype as that of SMI 81 and rhodamine-dextran (1:1) were used as a control.

The stair-step increases in FM1–43 uptake were better resolved by transforming our data to a differential over time (dy/dt; rate of dye uptake), which yielded profiles with identifiable upstrokes and downstrokes that could be analyzed subsequently by the PULSAR program [developed by Drs. Merriam, Kozuch, and Wachter, NICHHD, (Bethesda, MD), and University of California (Berkeley, CA)]. PULSAR enabled analysis of various pulsatile parameters, the most relevant of which were frequency and duration of peaks. Pulse amplitude was calculated from the original datasets as the difference between the areas under the curve defined by the three points following and preceding a pulse. Rises greater than 5% were considered significant deflections in FM1–43 incorporation (only 0.8% of pulses resolved by PC PULSAR analysis were rises smaller than 5% and were not considered significant pulses). To avoid false positives, we did not consider single point peaks as pulses in any of the FM1–43 profiles analyzed.

To quantify the degree of synchronization among cells within neuronal clusters, we compared the extent of synchronization with that expected if pulse coincidence were random. We used an algorithm model that consisted of a number of numeric channels corresponding to the number of cells in any given experiment. Each channel in the random model was comprised of a numeric series corresponding to the number of 5-min points in the related experimental dataset. Each time point in the random model was assigned a value based on the probability that a pulse would occur at that moment. Thus, the dataset generated for the random model paralleled that observed for the neurons, except that pulse concurrence was determined by random coincidence. This random model provided a measure of the extent to which random coincidence could be expected to occur during an experiment. Therefore, the predicted probability that more than 50% of the cells would display a pulse simultaneously was low and approached zero. We took this 50% to be a cut-off point for discrimination between random and nonrandom synchronization. The calculated index of synchronization (IOS) of pulses was, therefore, the ratio of pulse coincidence observed in more than 50% of cells to that predicted by the random model. Accordingly, a value of 1 indicated that true synchronization was low, because pulse coincidence in the experimental dataset was not different from that expected for random concurrence. The effect of time in culture on synchronization of secretory pulses was evaluated by comparing IOSs for neurons cultured less than 5 days with those cultured for at least 5 days. Under both culture conditions, clusters of neurons exhibiting more than 80% confluence were selected for study.

Statistical analysis

Statistical differences in frequency, duration, and amplitude of peaks in the absence or presence of nimodipine or octanol, and diffusion of LY toward neighboring cells in the absence or presence of octanol were assessed by one-way ANOVA, followed by the Newman-Keuls multiple comparison test. The time dependence of synchronization and the effects of nimodipine on this phenomenon were evaluated by one-way ANOVA followed by the Mann-Whitney U test. The effect of octanol on synchronization was assessed by one-way ANOVA, followed by unpaired Student's *t* test. All differences were considered statistically significant at $P < 0.05$.

Results

Monitoring of FM1–43 reveals pulsatility

Shown in Fig. 1A is a representative example of results obtained during long-term monitoring of FM1–43 uptake in individual GT1–7 neurons. Regardless of the degree to which individual neurons contacted one another, each cell exhib-

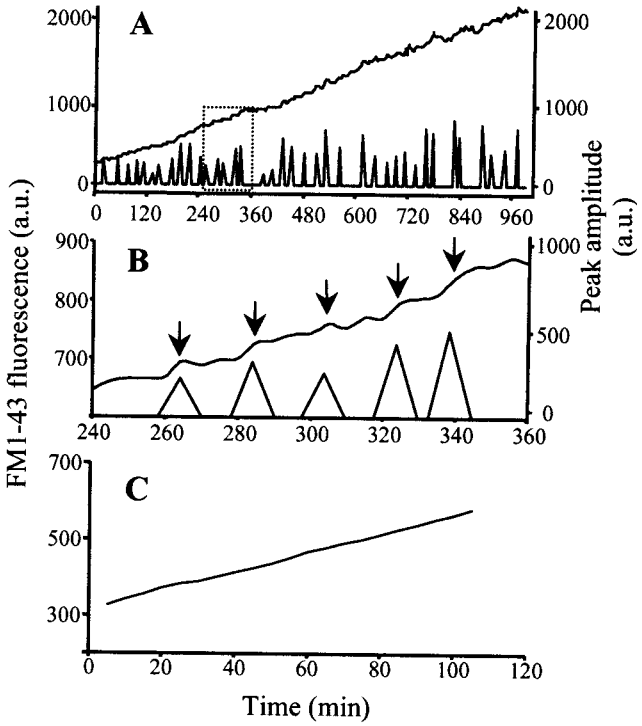

FIG. 1. Long-term measurements of FM1–43 uptake in individual GT1–7 cells. A, FM1–43 fluorescence of a cell representative of 16 (n = 9 experiments). The *upper line* shows the FM1–43 fluorescence profile of a cell sampled every 5 min. The *lower line* illustrates the frequency (determined from PC PULSAR) and the relative amplitude (calculated from the area under the FM1–43 profile) of pulses. The *dotted line box* encompasses a 2-h period that has been expanded (B) to observe in more detail the stepwise increments (*arrows*) in FM1–43 incorporation. C, Representative example of dye incorporation in a cell injected with SMI 81 (n = 4; 16 cells). Note that the intermittent stair-step increments of FM1–43 uptake displayed by noninjected cells disappeared in cells in which exocytosis was blocked by injection of SMI 81. The periodic pattern of FM1–43 incorporation in noninjected cells was not affected by injection of a nonspecific control IgG (n = 3; 16 cells). a.u., Arbitrary units in this and the following figures.

ited stepwise fluctuations of FM1–43 uptake or pulses. These fluctuations, which are illustrated more clearly in an expanded portion of the example (Fig. 1B), differed considerably from neuron to neuron. Indeed, these differences were manifested as changes in both frequency and amplitude of pulses. However, on the average, these cells displayed features of pulsatility (frequency, 1.4 ± 0.1 pulses/h; duration of peaks, 17.3 ± 0.6 min) comparable to those reported recently for entire cultures of perifused GT1–7 neurons (17). To further evaluate whether these stair-step increases in dye uptake were associated with exocytosis, we compared fluorescence profiles of normally secreting cells to those that had been injected with SMI 81, an antibody shown to arrest exocytosis in synaptosomal preparations (18). As illustrated (Fig. 1C), the frequency of stepwise increases in FM1–43 incorporation was strongly inhibited, with only an occasional pulse observed (0.17 ± 0.06 pulses/h; n = 4; 16 cells). Cells injected with the control antibody (1.2 ± 0.1 pulses/h; n = 3; 16 cells) were indistinguishable from noninjected controls (see above) and from temporally coincident noninjected controls (1.1 ± 0.1 pulses/h; n = 9; 12 cells). These results demonstrate that stair-steps increases in membrane fluorescence actually reflect endocytosis immediately following exocytotic bursts.

Effect of time in culture on synchronization of pulses among cells

Because of reports of functional changes in GT1 cells with time in culture (7), we compared the frequency, amplitude, and duration of pulses for cells cultured 2–4 days with those cultured at least 5 days. We found that all three parameters were very similar for both culture intervals analyzed (frequency, 1.5 ± 0.2 *vs.* 1.7 ± 0.1 pulses/h in cells cultured for <5 days and >5 days, respectively; amplitude, 550.0 ± 142.5 *vs.* 399.3 ± 78.2 arbitrary units, respectively; duration of peaks, 17.3 ± 0.6 *vs.* 15.6 ± 0.3 min, respectively; $P > 0.05$). However, the time in culture had a striking influence on interneuronal pulse synchronization. The pulses from multiple GT1–7 cells cultured for less than 5 days did not appear to be synchronized (Fig. 2A), whereas a strong coordinated relationship was evident in cultures maintained for at least 5 days, as evidenced by the intermittent, temporal overlap of pulses (Fig. 2B). Quantification of this relationship was achieved by comparing the IOS for the two groups. As shown in Fig. 2C, the IOS for cells maintained less than 5 days approached 1 (0.9 ± 0.1; n = 5 experiments), indicating that the degree of synchronization was not different from that predicted by a random model. In contrast, the IOS for cells cultured 5 days or more was 8.5 ± 2.2 (n = 7 experiments) or more than 8-fold higher than that expected to occur randomly. This difference in the IOS reveals that synchronized pulsatility is achieved only after several days in culture and indicates strongly that maturation of neuronal network communication is needed to attain this synchronized functional state. This effect on synchronization was not an artifact of cell density, because we selected fields in which the degrees of confluence (Fig. 2, D and E) were similar (80.5 ± 4.5% *vs.* 89.6 ± 3.7% in cells cultured for <5 and >5 days, respectively; $P > 0.05$).

Role of L-type calcium channels in the regulation of pulsatility and pulse synchronization

It has been reported that GT1–7 neurons display spontaneous intracellular free Ca^{2+} ($[Ca^{2+}]_i$) oscillations that are probably involved in the regulation of pulsatile hormone secretion (16, 19, 20). Influx of Ca^{2+} through L-type channels is at least in part responsible for the oscillatory nature of $[Ca^{2+}]_i$ mobilization in GT1–7 (19) and GT1–1 (21) cell lines. By using nimodipine [a specific L-type Ca^{2+} channel blocker at low concentrations (*e.g.* 0.1 μM)], we evaluated the role of Ca^{2+} influx through these channels in the regulation of pulsatility and synchronization in these cultures. GT1–7 neurons cultured for less than 5 days responded to administration of 0.1 μM nimodipine for 90 min with a striking decrease in the frequency (1.2 ± 0.1 *vs.* 0.6 ± 0.1 pulses/h for control and treated cells, respectively; $P < 0.05$) and amplitude (100.0 ± 21.0 *vs.* 44.6 ± 6.3% for control and treated cells, respectively; $P < 0.05$; n = 6 experiments; 48 cells) of pulses. However, when cells were maintained in culture for more than 5 days, nimodipine caused only a moderate reduction of these pul-

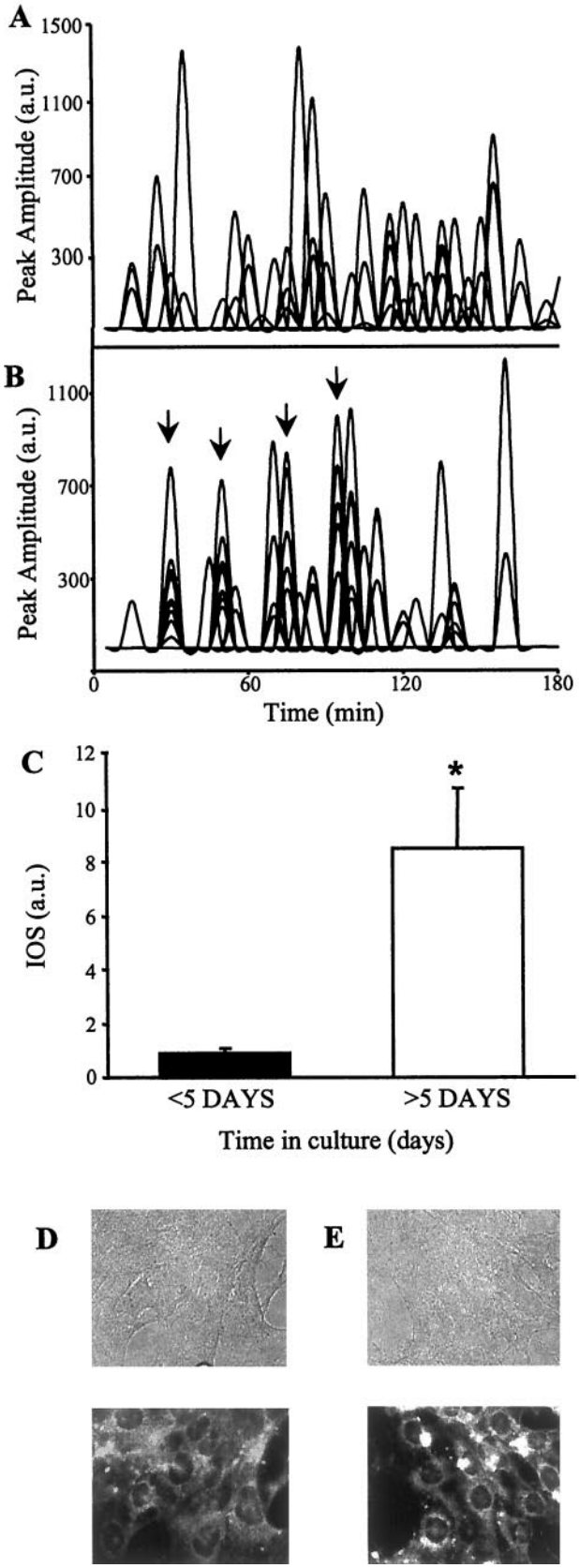

FIG. 2. Synchronized pulsatility as a function of time in culture. A, Representative example of the distribution of membrane changes associated with exocytosis displayed by 12 neurons within the same field and cultured for less than 5 days. As shown, very little overlap of pulses is evident. B, Representative example of the distribution of exocytotic events displayed by 15 neurons cultured for at least 5 days. After a critical period of culture, neurons coordinated their pulsatile activities to reveal high synchronization (overlap of pulses) at selected points in time (*arrows* indicate areas of extensive pulse overlap). C, IOS values (see *Materials and Methods*) of cells maintained in cultured for less than 5 days (■) and cells cultured for at least 5 days (□). These data are expressed as the mean ± SEM of five and seven independent experiments, respectively. *, $P < 0.05$ *vs.* cells cultured for less than 5 days. D and E, Phase (*upper*) and fluorescent (*lower*) images of GT1–7 neurons cultured for 3 (D) and 7 (E) days after 30 min of incubation with FM1–43 (×400). Note that the confluence of cells in both culture conditions is similar.

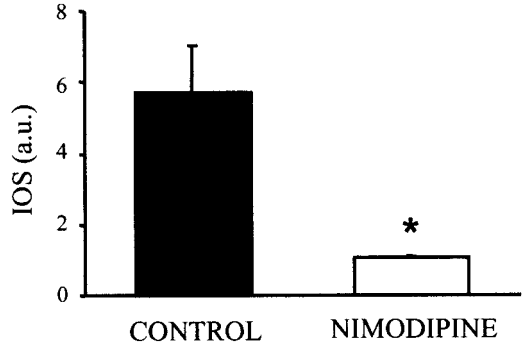

FIG. 3. Effect of nimodipine on pulse synchronization. Shown here are IOS values (see *Materials and Methods*) of cells that were maintained in culture for at least 5 days without (control conditions, ■) and with (□) 0.1 μM nimodipine for 90 min. Data are expressed as the mean ± SEM of 4 (48 cells) and 3 (28 cells) independent experiments, respectively. *, $P < 0.05$ *vs.* control conditions.

satile parameters (frequency, 1.5 ± 0.1 *vs.* 1.1 ± 0.2 pulses/h; amplitude, 100.0 ± 6.2% *vs.* 87.2 ± 5.4%; $P > 0.05$; n = 3 experiments; 88 cells). In contrast to the modest diminution exerted on intrinsic pulsatility, nimodipine abolished the synchronization of pulses among neighboring GT1–7 cells cultured for more than 5 days (Fig. 3). These results demonstrate clearly that the influx of Ca^{2+} through L-type channels is not only involved in intrinsic pulsatility, but is also required for synchronization of these pulses.

Role of gap junction functionality in the synchronization of pulses

Our demonstration of synchronized pulse profiles among cells begs the question of how this communication is achieved. Inasmuch as gap junctions are reported to exist in GT1–7 neurons (12, 13, 22), and they (23) or their corresponding proteins (24) have been found in hypothalamic GnRH neurons, these structures seemed a logical candidate to subserve a coordinating role. Accordingly, we tested for the presence of functional gap junctions in nonsynchronized and synchronized cells by monitoring LY dye transfer among adjacent cells under conditions where cell density was constant (78.3 ± 4.5 and 80.6 ± 5.9 cells/region before and after 5 days in culture, respectively; $P > 0.05$). As shown in Fig. 4A, we found that diffusion of dye in nonsynchronized (<5 days in culture) cells was limited, as evidenced by the fact that each LY-staining cell was also stained with rhodamine. Because rhodamine is conjugated to dextran and cannot pass

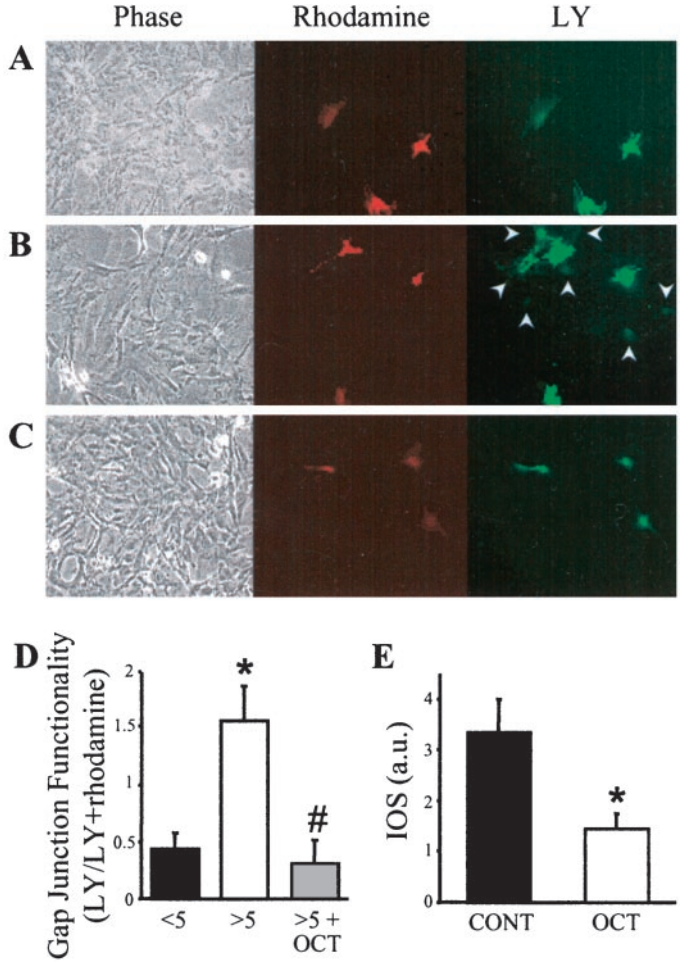

FIG. 4. Influence of time in culture and octanol treatment on dye transfer in GT1–7 cells. GT1–7 cells cultured for less than 5 days (A), more than 5 days (B), and more than 5 days with octanol added for the last 30 min of culture (C) were compared. Microscopic images with phase contrast (*left column*), the rhodamine dextran fluorescent emission (*center column*), and the LY fluorescent emission (*right column*) are presented (×100). *Arrowheads* delineate cells to which LY diffused. D, Shown here are the indexes of gap junction functionality (see *Materials and Methods*) in neurons cultured for less than and more than 5 days (■ and □, respectively; n = 4 experiments; 24 regions of interest) and those cultured for more than 5 days and incubated with octanol for the last 30 min of culture (▩; n = 3 experiments; 22 regions of interest). *, $P < 0.05$ *vs.* cells cultured for less than 5 days. #, $P < 0.05$ *vs.* cells cultured for more than 5 days. Note that the diffusion of LY to adjacent cells through gap junctions was more extensive in cells cultured for at least 5 days. The blockade of gap junctions with octanol inhibited the transfer of dye to adjacent cells. E, The blockade of gap junctions was also reflected in the synchronization of secretory pulsatility. Presented here are the IOS values (see *Materials and Methods*) of synchronized cells cultured for at least 5 days (control conditions, ■) and synchronized cells incubated with 20 μM octanol for 30 min (□). Data are expressed as the mean ± SEM of 5 independent experiments. *, $P < 0.05$ *vs.* control conditions.

through gap junctions, this costaining would indicate that LY is present only in the cells originally injected. In contrast, many cells in synchronized cultures (>5 days in culture) were stained with LY (Fig. 4B, *arrowheads*), but not rhodamine, revealing that diffusion had occurred (Fig. 4B). Interestingly, treatment of these synchronized cultures with octanol (20 μM), which is known to specifically block junctional conductance (25), severely reduced the transfer of dye (Fig. 4C). These relationships are illustrated more quantitatively in Fig. 4D. Notably, the degree of gap junction functionality was about 4-fold greater for synchronized (cultured for >5 days) *vs.* nonsynchronized (cultured for <5 days) cells, and treatment with octanol abolished this difference. These results demonstrate that octanol can inhibit functionality of gap junctions in GT1–7 neurons. Additionally, the ability of octanol to inhibit gap junction communication was accompanied by an inhibition of synchronization among cells. The IOS found after administration of octanol was about 2-fold lower than that exhibited by GT1–7 cells under control conditions (Fig. 4E). Thus, it appears that functional gap junctions are necessary for cell-cell communication and that this form of communication underlies the synchronization of pulsatility in GT1–7 cell populations. It must be emphasized, however, that the ability of an individual cell to pulse is not dependent on gap junctions. This is evidenced by the observation that cells in the absence or presence of octanol exhibited similar frequency (1.8 ± 0.1 *vs.* 1.9 ± 0.2 pulses/h, respectively; $P > 0.05$), amplitude (723.8 ± 269.7 *vs.* 764.2 ± 183.5 arbitrary units, respectively; $P > 0.05$) and duration of pulses (18.9 ± 1.7 *vs.* 17.6 ± 2.1 min, respectively; $P > 0.05$).

Discussion

The intermittent release of GnRH from the hypothalamus is absolutely necessary for proper reproductive function (1). A growing body of evidence indicates that this pulsatile pattern of GnRH release is controlled *in vivo* by a mechanism that is relatively independent of extrahypothalamic input. Instead, pulsatility has been proposed to be an intrinsic property of the neurons themselves (1, 26, 27), but the cellular basis for this phenomenon has remained elusive (2). In particular, it has been difficult to discern whether episodic GnRH secretion was driven purely by single cell mechanisms common to individual neurons or whether it depended upon the ability of neurons to communicate within a neuronal network. The capacity to distinguish between the validity of intrinsic (7–10) as opposed to network-dependent (6, 12, 13) models for pulsatile release has been hindered because available evidence was derived from population studies, in which the averaged responses of tens of thousands of cells were measured. By contrast, in the current study we used a novel approach, membrane incorporation of FM1–43 fluorescent dye, to resolve single cell secretory dynamics among individual neurons in a population. Initially in the last decade, FM1–43 has been used to investigate trafficking of vesicles to the plasma membrane and endocytotic recycling (28). More recently, the use of FM1–43 uptake as an indirect marker of exocytosis was explored (16, 29). During exocytosis, secretory granules fuse to the plasma membrane, providing new membrane into which this fluorescent dye can incorporate. Endocytosis which follows an exocytotic event brings these newly labeled membranes into the cell, thereby increasing the total fluorescent signal. Because of the complexity of this process, there has been certain controversy about the ability of this dye to discriminate between reuptake of recently exocytosed membrane or constitutive and receptor-mediated endocytosis. Specific blockage of stair-step in-

creases in membrane fluorescence by cytoplasmic injections of anti-SNAP 25 [a protein necessary for the fusion of secretory granules to the plasma membrane (30)] provides strong evidence that each of these increases measured in GT1–7 cells is associated with a single exocytotic burst. Further, our use of this approach in the present study enabled us to confirm that pulsatile changes in FM1–43 incorporation occur spontaneously and change dynamically over time. Although each neuron pulsed in a rhythmic fashion, our results revealed that pulses of secretion were heterogeneous (in terms of frequency and amplitude) and differed in timing among neighboring GT1–7 neurons. These results suggest strongly that each cell functions independently and that these pulses are an intrinsic property of each cell in the culture population.

Our initial results made it very difficult to understand the manner in which these individual units could function in harmony until we observed that this individual neuronal activity came to be coordinately regulated after a fixed time in culture. Because this coordination did not appear to be a function of cell density, we reasoned that it reflected a maturational or differentiational process required for establishment of a functional neuronal network. Possible mechanisms that have been associated with GnRH cell function and could provide the necessary degree of signal concurrence required for synchronization include paracrine messengers, synaptic connections, and communication through gap junctions (for review, see Ref. 31). Because of identification of functional gap junctions or proteins related to these communication structures in GT1–7 cells (12, 13, 22) and the ability of gap junctions to transmit a coordinating signal among adjacent cells in a fast and effective manner, we directed our efforts to explore the participation of gap junctional communication in the maintenance of coordinated exocytosis among GT1–7 cells.

Our next series of experiments involved the use of fluorescent dyes to determine the degree of gap junctional communication between GT1–7 cells. Our ability to abolish synchronization of pulsatile activity by treatment with the gap junction inhibitor octanol demonstrates for the first time that this form of cell communication is an absolute requirement for concerted pulsatility in GT1–7 neurons. From a functional point of view, gap junctions are permeable to a variety of different secondary metabolites and intracellular ions, any of which might convey the coordinating signal required for synchronization. Included among these are cAMP (32), Ca^{2+}, inositol trisphosphate (32–35), Na^{+}, K^{+}, and cADP-ribose (34), but at this time, it is not known which (if any) of these is involved in synchronization of pulsatility in GnRH neurons. A recent intriguing hypothesis (36), which holds that cAMP and associated signaling events comprise an oscillatory timing mechanism in single GT1 neurons, coupled with the capacity of this nucleotide to traverse gap junctions make it a particularly strong candidate to drive both inherent and synchronized pulsatility.

Our current observations also appear to more clearly define the cellular basis for secretory pulsatility. The ability of octanol to abolish synchronization of pulsatile release patterns was in stark contrast to its lack of effect on the episodic pulsatility measured in individual GT1–7 neurons. Remarkably, the frequency, duration, and amplitude of pulsatile episodes in single cells were unaffected. Thus, in addition to defining the central role of gap junctions in synchronization, these observations also provide compelling evidence to support the conclusion that synchronization and pulsatility are to a certain extent mutually exclusive and independent processes. Indeed, the distinct ability of octanol to abolish synchronization without effects on single cell pulsatile secretory activity implies that the former depends entirely on junctional network communication and the latter does not.

Intriguingly, we found that nimodipine, an L-type, voltage-gated Ca^{2+} channel blocker, exerted differential effects on GT1–7 neurons depending on whether they were cultured sufficiently long to achieve synchronization. In cells cultured for less than 5 days (nonsynchronized cells), nimodipine severely attenuated pulse frequency and amplitude. The ability of nimodipine to reduce these parameters was minimized in cells that were already synchronized, demonstrating a difference in the extent to which L-type calcium channels contributed to secretory pulsatility before and after neurons were fully differentiated. Moreover, the modest partial inhibitory effect of nimodipine on pulsatile activity in single cells paled in comparison with its dramatic inhibition of synchronization. As was the case for the differential effects of octanol described above, this observation reinforces our proposal that inherent pulsatility and synchronization are fundamentally independent processes. The requirement of functional L-type channels for pulse synchronization raises the question of what mechanistic role they play. Inasmuch as we have demonstrated the necessity of gap junctions for synchronization, we must speculate further that action potential propagation could occur via bidirectional monovalent cationic flux through gap junctions. Presumably, the resulting depolarization in adjoining cells would lead to L-type calcium channel opening and further activation of calcium spiking activity. The initiation of L-type calcium channel activity could lead to a synchronized release of GnRH.

In summary, we have demonstrated clearly that the individual cell is the functional unit responsible for elaboration of pulsatility in cultures of GT1–7 neurons. The lack of LY dye transfer or octanol influence on pulsatile activity in nonsynchronized cells coupled with the paucity of evidence for other types of rapid communication between GT1–7 cells indicate that pulsatility within a given neuron does not require cell-cell communication. Moreover, we have also demonstrated that concurrence of secretory pulses among adjacent neurons relies upon the development of gap junctional channels that provide for synchronized communication. Taken together, our results indicate that two components, intrinsic cellular pulsatility and cell-cell communication, are responsible for the elaboration of synchronized secretory pulses from populations of GT1–7 cells. Our findings, when viewed in light of the extensive functional similarities between these clonal cells and hypothalamic GnRH-secreting neurons, lend credence to the possibility that these two components form the cellular basis for the elusive GnRH pulse generator in the hypothalamus.

Acknowledgments

We thank William J. Faught and David C. Leaumont for expert technical assistance. We are indebted to Dr. Richard I. Weiner (University of California-San Francisco) for his generous gift of the GT1–7 cells.

References

1. **Terasawa E** 1995 Control of luteinizing hormone-releasing hormone pulse generation in nonhuman primates. Cell Mol Neurobiol 15:141–164
2. **Terasawa E** 1998 Cellular mechanism of pulsatile LHRH release. Gen Comp Endocrinol 112:283–295
3. **Silverman AJ, Jhamandas J, Renaud LP** 1987 Localization of luteinizing hormone-releasing hormone (LHRH) neurons that project to the median eminence. J Neurosci 7:2312–2319
4. **Knobil E** 1980 The neuroendocrine control of the menstrual cycle. Recent Prog Horm Res 36:53–88
5. **Mellon PL, Windle JJ, Goldsmith PC, Padula CA, Roberts JL, Weiner RI** 1990 Immortalization of hypothalamic GnRH neurons by genetically targeted tumorigenesis. Neuron 5:1–10
6. **Krsmanovic LZ, Stojilkovic SS, Merelli F, Dufour SM, Virmani MA, Catt KJ** 1992 Calcium signaling and episodic secretion of gonadotropin-releasing hormone in hypothalamic neurons. Proc Natl Acad Sci USA 89:8462–8466
7. **Krsmanovic LZ, Martinez-Fuentes AJ, Arora KK, Mores N, Navarro CE, Chen HC, Stojilkovic SS, Catt KJ** 1999 Autocrine regulation of gonadotropin-releasing hormone secretion in cultured hypothalamic neurons. Endocrinology 140:1423–1431
8. **Weiner RI, Wetsel W, Goldsmith P, Martinez de la Escalera G, Windle J, Padula C, Choi A, Negro-Vilar A, Mellon P** 1992 Gonadotropin-releasing hormone neuronal cell lines. Front Neuroendocrinol 13:95–119
9. **Martinez de la Escalera G, Choi AL, Weiner RI** 1992 Generation and synchronization of gonadotropin-releasing hormone (GnRH) pulses: intrinsic properties of the GT1–1 GnRH neuronal cell line. Proc Natl Acad Sci USA 89:1852–1855
10. **Martinez de la Escalera G, Choi AL, Weiner RI** 1995 Signaling pathways involved in GnRH secretion in GT1 cells. Neuroendocrinology 61:310–317
11. **Masotto C, Negro-Vilar A** 1988 Gonadectomy influences the inhibitory effect of the endogenous opiate system on pulsatile gonadotropin secretion. Endocrinology 123:747–752
12. **Matesic DF, Germak JA, Dupont E, Madhukar BV** 1993 Immortalized hypothalamic luteinizing hormone-releasing hormone neurons express a connexin 26-like protein and display functional gap junction coupling assayed by fluorescence recovery after photobleaching. Neuroendocrinology 58:485–492
13. **Matesic DF, Hayashi T, Trosko JE, Germak JA** 1996 Upregulation of gap junctional intercellular communication in immortalized gonadotropin-releasing hormone neurons by stimulation of the cyclic AMP pathway. Neuroendocrinology 64:286–297
14. **Angleson JK, Cochilla AJ, Kilic G, Nussinovitchm I, Betz WJ** 1999 Regulation of dense core release from neuroendocrine cells revealed by imaging single exocytic events. Nat Neurosci 2:440–446
15. **Cochilla AJ, Angleson JK, Betz WJ** 2000 Differential regulation of granule-to-granule and granule-to-plasma membrane fusion during secretion from rat pituitary lactotrophs. J Cell Biol 150:839–848
16. **Nuñez L, Villalobos C, Boockfor FR, Frawley LS** 2000 The relationship between pulsatile secretion and calcium dynamics in single, living gonadotropin-releasing hormone neurons. Endocrinology 141:2012–2017
17. **King TS, Potter D, Kang IS, Norris C, Chen E, Schenken RS, Javors MA** 1999 Concentration-dependent effects of muscimol to enhance pulsatile GnRH release from GT1–7 neurons in vitro. Brain Res 824:56–62
18. **Mehta PP, Battenberg E, Wilson MC** 1996 SNAP-25 and synaptotagmin involvement in the final Ca^{2+}-dependent triggering of neurotransmitter exocytosis. Proc Natl Acad Sci USA 93:10471–10476
19. **Charles AC, Hales TG** 1995 Mechanisms of spontaneous calcium oscillations and action potentials in immortalized hypothalamic (GT1–7) neurons. J Neurophysiol 73:56–64
20. **Hales TG, Sanderson MJ, Charles AC** 1994 GABA has excitatory actions on GnRH-secreting immortalized hypothalamic (GT1–7) neurons. Neuroendocrinology 59:297–308
21. **Costantin JL, Charles AC** 1999 Spontaneous action potentials initiate rhythmic intercellular calcium waves in immortalized hypothalamic (GT1–1) neurons. J Neurophysiol 82:429–435
22. **Hu L, Olson AJ, Weiner RI, Goldsmith PC** 1999 Connexin 26 expression and extensive gap junctional coupling in cultures of GT1–7 cells secreting gonadotropin-releasing hormone. Neuroendocrinology 70:221–227
23. **Suter KJ, Wuarin JP, Smith BN, Dudek FE, Moenter SM** 2000 Whole-cell recordings from preoptic/hypothalamic slices reveal burst firing in gonadotropin-releasing hormone neurons identified with green fluorescent protein in transgenic mice. Endocrinology 141:3731–3736
24. **Hosny S, Jennes L** 1998 Identification of gap junctional connexin-32 mRNA and protein in gonadotropin-releasing hormone neurons of the female rat. Neuroendocrinology 67:101–108
25. **Veenstra RD, DeHaan RL** 1986 Measurement of single channel currents from cardiac gap junctions. Science 29:972–974
26. **Bourguignon JP, Franchimont P** 1981 Intermittent liberation of gonadoliberin (GnRH) by the rat hypothalamus *in vitro*. C R Seances Soc Biol Fil 175:389–396
27. **Bosma MM** 1993 Ion channel properties and episodic activity in isolated immortalized gonadotropin-releasing hormone (GnRH) neurons. J Membr Biol 136:85–96
28. **Cochilla AJ, Angleson JK, Betz WJ** 1999 Monitoring secretory membrane with FM1–43 fluorescence. Annu Rev Neurosci 22:1–10
29. **Stafford SJ, Shorte SL, Schofield JG** 1993 Use of a fluorescent dye to measure secretion from intact bovine anterior pituitary cells. Biosci Rep 13:9–17
30. **Sollner T, Bennett MK, Whiteheart SW, Scheller RH, Rothman JE** 1993 A protein assembly-disassembly pathway in vitro that may correspond to sequential steps of synaptic vesicle docking, activation, and fusion. Cell 75:409–418
31. **Wetsel WC** 1995 Immortalized hypothalamic luteinizing hormone-releasing hormone (LHRH) neurons: a new tool for dissecting the molecular and cellular basis of LHRH physiology. Cell Mol Neurobiol 15:43–78
32. **Kam Y, Kim DY, Koo SK, Joe CO** 1998 Transfer of second messengers through gap junction connexin 43 channels reconstituted in liposomes. Biochim Biophys Acta 1372:384–388
33. **Kandler K, Katz LC** 1998 Coordination of neuronal activity in developing visual cortex by gap junction-mediated biochemical communication. J Neurosci 18:1419–1427
34. **Churchill G, Louis C** 1998 Roles of Ca^{2+}, inositol trisphosphate and cyclic ADP-ribose in mediating intercellular Ca^{2+} signaling in sheep lens cells. J Cell Sci 111:1217–1225
35. **Hofer T** 1999 Model of intercellular calcium oscillations in hepatocytes: synchronization of heterogeneous cells. Biophys J 77:1244–1256
36. **Vitalis EA, Costantin JL, Tsai PS, Sakakibara H, Paruthiyil S, Iiri T, Martini JF, Taga M, Choi AL, Charles AC, Weiner RI** 2000 Role of the cAMP signaling pathway in the regulation of gonadotropin-releasing hormone secretion in GT1 cells. Proc Natl Acad Sci USA 97:1861–1866